4. Vijaykumar, Joseph, A., Prabhudesai, R. G., Prabhudesai, S., Nagvekar, S. and Damodaran, V., Performance evaluation of Honeywell silicon piezoresistive pressure transducers for oceanographic and limnological measurements. *J. Atmos. Ocean. Technol*., 2005, **22**, 1933–1939.
5. Joseph, A., Mehra, P., Odametey, J. and Nkebi, E. K., Pressure gauge based GLOSS sea level station at Takoradi harbour (Ghana, West Africa) – Experiences over a year. In *IOC Manual on Sea Level Measurement and Interpretation*, 2006, vol. 4 (an update to 2005), pp. 108–110.
6. Gieles, A. C. M. and Somers, G. H. J., Miniature pressure transducers with a silicon diaphragm. *Philips Tech. Rev*., **33**, 14–20.
7. Joseph, A., Desa, E., Desa, E. S., Smith, D., Peshwe, V. B., Kumar, V. and Desa, J. A. E., Evaluation of pressure transducers under turbid natural waters. *J. Atmos. Ocean. Technol.*, 1999, **16**, 1150–1155.
8. Joseph, A., Desa, E., Kumar, V., Desa, E. S., Prabhudesai, R. G. and Prabhudesai, S., Pressure gauge experiments in India. Intergovernmental Oceanographic Commission Workshop Report No. 193, Workshop on New Technical Developments in Sea and Land Level Observing Systems (eds Holgate, S. and Aarup, T.), 14–16 October 2003, Paris, France, 2004, pp. 22–37.
9. Joseph, A., Modern techniques of sea level measurement. In *Encyclopaedia of Microcomputers*, Marcel Dekker, New York, 1999, vol. 23, pp. 319–344.
10. Joseph, A. and Prabhudesai, R. G., Web-enabled and real-time reporting cellular based instrumentation for coastal sea level and surge monitoring. In *The Indian Ocean Tsunami* (eds Aswathanarayana, U. and Tad Murthy), A. A. Balkema Publishers, Taylor & Francis Group, Leiden, The Netherlands, 2006, in press.

ACKNOWLEDGEMENT. Support provided by *INS Mandovi* in erecting the gauge at Verem Jetty, Goa is acknowledged.

Received 16 October 2005; revised accepted 6 February 2006

Imaging trench-line disruptions: swath mapping of the Andaman subduction zone

Bishwajit Chakraborty and Ranadhir Mukhopadhyay*

National Institute of Oceanography, Dona Paula, Goa 403 004, India

Analogous to other subduction zones in the world where the heavier oceanic plate shoves below the lighter continental plate, crustal movement along the Sumatra–Andaman trench line over the last two centuries released enormous stress causing earthquakes of highest impunity and generating, at times, devastating tsunamis. Such significant earth movements are presumed to have wide-ranging implications, stretching from geology to climate and to astronomy. A sea expedition within three months from the 2004 Sumatra–Andaman earthquake, and during the 2005 Sumatra earthquake is able to image the exact trench line, west of the Andaman Island. The multibeam bathymetry, gravity and fractal studies of about twenty-five thousand square kilometres off the west of Andaman Island have brought out several interesting features unknown earlier, including atypical disruption of the trench line.

Keywords: Disruption, subduction zone, Sumatra–Andaman earthquake, trench line.

THE M_w 9.0–9.3 Sumatra earthquake of 26 December 2004 (26/12), the most severe among the top nine earthquakes reported during the last two hundred years (Table 1), occurred at the shallow interface in near proximity to four plates – two oceanic (Indian, Australian) and two continental (Burma and Sunda)[1]. This earthquake (epicentre location 3.3°N, 96°E; focal depth 30 km) was probably the first such major phenomenon that was recorded with modern equipment such as satellites offering information on ocean heights, in addition to a global seismic network with seismographs and a networking of global positioning system (GPS) to document even minor crustal movements[2]. The distribution of aftershocks suggests progressive rotation of the strike of the fault plane towards right as the rupture progressed towards north[3], implying increase in strike slip component towards north. Again, as recorded by seismometers in Russia and Australia, in the beginning the crust broke 100 km patch slowly, then rapidly to 3 km/s for the next 4 min, and thereafter maintained an average speed of 2.5 km/s for the next 6 min (average rupture speed 8050 km/h)[4].

Analysis of regional geodetic (GPS) data further suggests that a highly oblique motion between Indo-Australian and Burma–Sunda plates is partitioned between the trench normal thrust motion at the subduction zone in the Sumatra region to arc-parallel dextral strike-slip faulting off the Andaman Islands[5]. The enormity of the earthquake, considered to have been initiated at a depth of about 30–40 km below the seafloor, has been so huge that almost 0.25 million km^2 of the crust in the subduction zone was estimated to have been ruptured[6], raising the Burma plate

Table 1. Historical seismic ($Mw > 7.0$) and volcanic activities along Andaman–Sumatra subduction zone

Year	Intensity	Area	Remarks
2005	*M* 8.6	Sumatra–Andaman	Major quake
2004	*M* 9.3	Sumatra–Andaman	Tsunami
2002	*M* 7.2	Ache, Sumatra	Major quake
1941	*M* 7.9	Andaman Island	Tsunami
1907	*M* 7.8	North-northcentral Sumatra	Tsunami
1883	–	Krakatoa volcanic eruption	Tsunami
1881	*M* 7.9	Nicobar Island	Tsunami
1861	*M* 8.5	Northcentral Sumatra	Major quake
1833	*M* 9.3	South Sumatra	Major quake
1797	*M* 8.4	Southcentral Sumatra	Major quake

Source: United States Geological Survey website.

*For correspondence. (e-mail: ranadhir@nio.org)

by about 10 m along a fault traversing for more than 1000 km between Sumatra and Andaman[2]. The width of the rupture zone is estimated to be about 150 km, with maximum slip[7] along the trench line being 10–20 m.

The enormity of 26/12 once again proved that the scientific community knows little of the mechanism and consequences of this sort of natural phenomenon. It was then felt that a detailed *in situ* imaging of the trench line would probably offer some interesting information. Accordingly, a sea expedition onboard ORV *Sagar Kanya* was arranged within three months from 26/12 (expedition SK 218, 18 March–16 April 2005). While the expedition was on, the Nias earthquake of 28 March 2005 occurred and the shuddering effect was felt onboard. The expedition covered a large area and undertook geological and geophysical investigations in the proximity of the trench and its surroundings. Detailed multibeam swath bathymetry investigation carried out during the expedition finds likely signatures of intense crustal movement off the Andaman Islands. The area surveyed is about 875 km NNW of the main epicentre of the 26/12 earthquake and includes from west to east the abyssal plain, part of submerged Ninetyeast Ridge, the subduction trench area, and the western slope of the sharply erected Andaman Ridge (Figure 1). The survey area represents the northern extension of the 1000 km long zone reportedly affected by 26/12. The survey area incidentally also constitutes a vital link between the Sunda arc towards the south and the Himalayan collision zone in the north through the Burmese arc[8].

The trench line in the Andaman subduction zone that trends NNE–SSW is long and narrow. This has been developed over a period of time and was naturally disturbed by the events of subduction-related earthquakes. In fact, nine violent earthquakes ranging in intensity between 7.2 and 9.4 have been recorded along this subduction zone during the last two centuries (Table 1). At least in four instances these earthquakes caused tsunamis. The fifth tsunami in this region was caused by the eruption of Krakatoa volcano. The trench is sharply delineated on the east by piled-up under-thrusted sediment scraped from the top surface of the subducting Indian plate (red-brown shaded area, Figure 1). The resulting en-echelon piling of sediments forms the Andaman Ridge, at the top sub-aerial part of which the Andaman group of Islands is located. The deepest part along this sediment-filled trench within the survey area is located at little more than 3900 m. The ridge and the trench are broken in their trend by the centre, indicating a clear signature of stress-induced dislocation. Although considered in earlier studies as a largely continuous curved feature with eastward concavity[8,9] (inset, bottom left, Figure 1), the Andaman Trench, as revealed in this study, is a discontinuous trench and is broken at least in three places within the survey area (Figure 1). These breaks are roughly located at latitudes 11°42′N, 12°25′N and 12°55′N.

The broken sections range in length from about 22 km in the south (incomplete by the limit of the exploration block of the present study) to 80 and 64 km in successive sections towards north within the survey area. The nearly north-south running trench line could be divided into four well-identified sections depending on the nature of disruptions. For example, the 26 km long southernmost section of the disrupted trench line shows a moderately steep western slope and a gently sloping wide eastern flank. The trench here is located at a depth between 3600 and 3900 m, with the bulged ridge on the east rising to about 1500 m. The next disrupted section to the north is approximately 86 km long and extends between 11°35′N and 12°25′N. This sickle-shaped trench (at places concave towards west) shows a slight shift in its disposition by a couple of kilometres towards west and is bordered on the east by a sharply elevated 1100 m high linear ridge. At times, the depth of the trench reaches beyond 3700 m.

The third disrupted section towards north extends between 12°15′N and 12°55′N and runs for about 77 km in a north-south direction. In general, this section shows an arcuate sickle-type dispensation, convex towards west. The trench appears deepest in this subsection (>3600 m) with nearly vertical western flank (high slope angle) and gentle eastern flank. The relatively undisturbed section of the trench line is located north of 12°50′N and runs for about 83 km till cut short by the northern extension of the present survey area. Showing concavity towards east with a smooth curve, the thickness of the trench line along the length of this section widens to a range between 2.5 and 6 km. The trench is deeper in the north compared to its southern part.

Interestingly, the broken sections of the disrupted trench line overlap each other at several places. The length of the overlapping arms ranges from about 10 to 13 km, with distance between the overlapping arms varying from 6 to 10 km. For example, the two southern sections overlap for a length of about 13 km, with overlapping arms separated by about 6 km, while two northern sections overlap for a length of little more than 12 km, with distance between two overlapping arms about 8 km. The length of and distance between the overlapping arms between the second and third sections from the south remain at about 10 km. All the tearing and dislocation of the trench line at the subduction zone occurred due to crustal movements over the years (Table 1), which are also reported through a recent visit to this area[7].

Free-air, Bouger gravity and total gravity data were collected from the survey area. Later, a 2D contour and 3D perspective maps were prepared from these data. A relatively low free-air gravity value was encountered all along the trench line, ranging from 115 to 125 mGal. The surrounding seafloor on either side, including the ridges, however, shows comparatively high free air gravity values ranging between 135 and 160 mGal. Regionally, a much higher value (180–190 mGal) over a NNE–SSW trending long feature about 50 km to the west of the Andaman trench was encountered. When examined in regional physi-

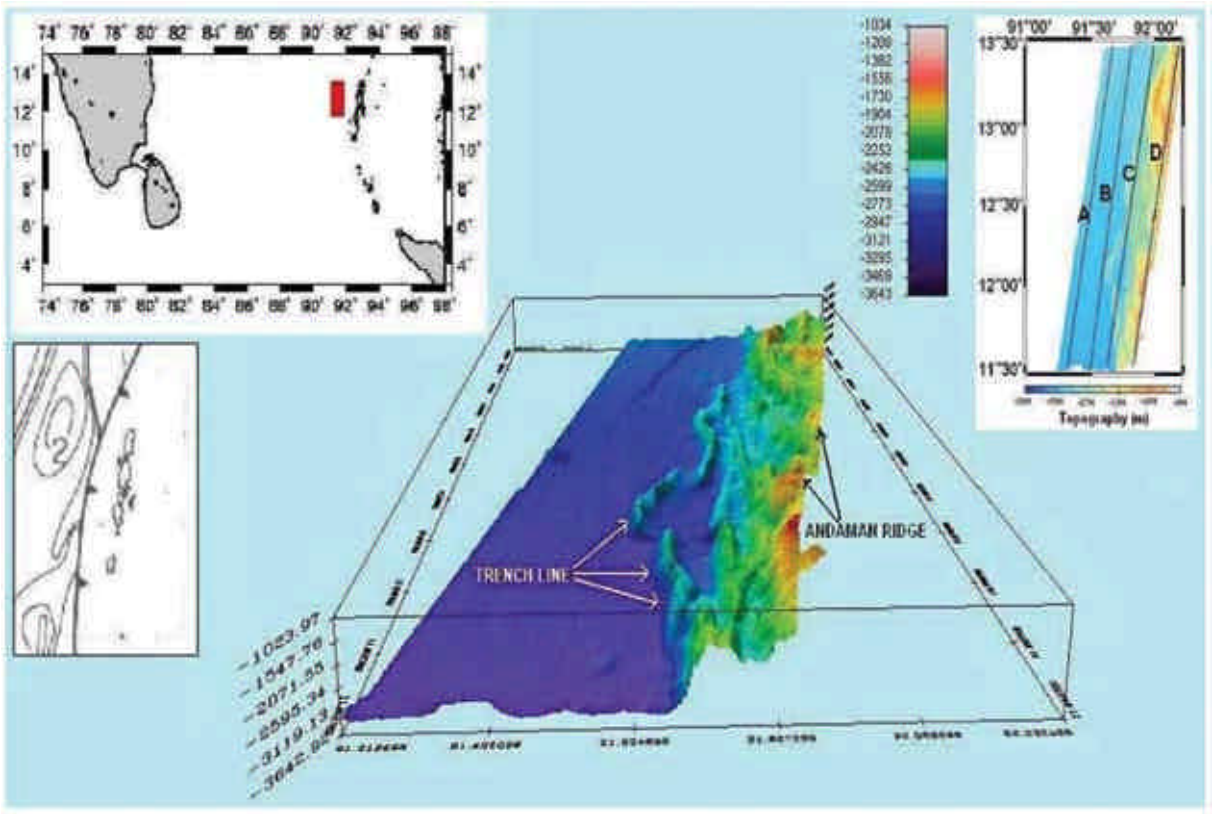

Figure 1. 3D seafloor map of the Andaman subduction zone based on data obtained from multibeam (59 beams) bathymetry system. Note dislocated and overlapping trench line. (Inset, top left) Survey area shown as red rectangle. (Inset, bottom left) Earlier assessment shows a gently curved Andaman trench line[8]. (Inset, right) Profiles A–D.

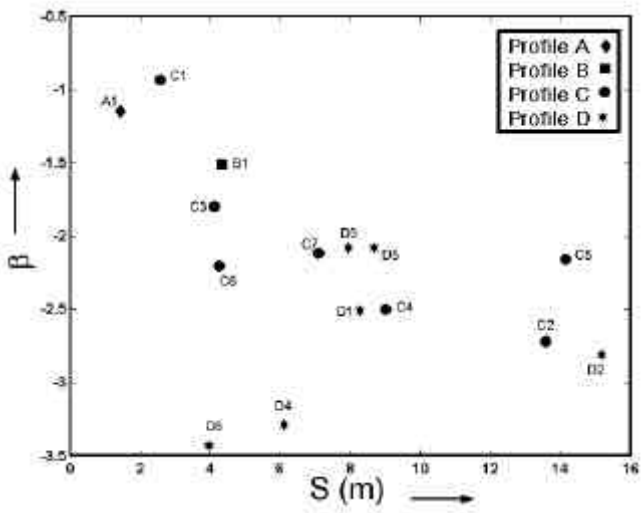

Figure 2. Fractal studies of Andaman subduction zone geomorphology. Note scattering of bathymetry segments along profile C, which runs over the trench line. Data indicate a stressed seafloor combining extreme variations in bathymetry.

ographic settings, it points to the possible presence of the buried Ninety East Ridge. This buried ridge distinctly maintains a positive free-air gravity anomaly throughout its length.

Our estimation of spectral exponent (b) and amplitude (S) using multi-beam bathymetry data helps quantify variations in seafloor morphology of the surveyed area. Generally, low b corresponds to rough seafloor, while S quantifies overall energy at a given area, i.e. for profiles having similar b but higher S will correspond to rougher profile. We extracted four evenly spaced depth-grid profiles (A–D, inset, Figure 1), along which power law parameter is obtained using smooth periodogram approach. Segmentation of the profiles into stationary intervals is made before spectral parameter estimation. The input profile is de-trended, freed from edge effect or leakage and subjected to Fast Fourier Transform (FFT) algorithm to achieve sample power spectrum periodogram.

The seafloor along the profiles A and B lacks variations and hence could not be divided into segments. Based on strikingly distinguishable topographical variations, profiles C and D are divided into thirteen segments. Large-scale roughness dominates along the profile D (b = –2.1 to –3.5, and S = 4 to 15.5). Interestingly, profile C exhibits comparatively higher ranges of variations along its seven segments (b = –1 to –2.75, and S = 2 to 14; Figure 2), which may be due to irregular disruption of the subduction zone (shifting of trench line?) and may indicate uneven causal stress condition. Such an incident of shifting of

trench line has occurred also during the 26/12 earthquake. For example, geodetic data recorded through global positioning system show a WSW to southwestwards smaller shift of trench line by about 4.8 m of the Andaman Islands, and a relatively larger shift by about 6.5 m towards south off the Nicobar region[10].

The western coastline of the Andaman–Nicobar Island is fairly straight and gentle in comparison to the notch and ophiolite-bearing eastern coastline[8]. Tilting and gradual submergence of the island group westwards and consequent uplift of the Andaman Ridge since early Oligocene–Late Eocene, probably facilitated formation of the barrier reef along the west coast[9]. Our 3D studies underway add to this understanding, showing dislocation and shifting of the Andaman subduction trench line towards west. This conforms to the earlier assessment[8,9] for a general westward shift of the Andaman trench with every episode of subduction of the plate. Furthermore, the continuing aftershocks and recent volcanism suggest that the geodynamics in the arc areas of the Sumatra–Andaman belt is undergoing significant changes. It is time a holistic assessment of the entire Asian plate geometry is made.

1. Mukhopadhyay, R. and De, S., Dealing with 26/12. *Curr. Sci*., 2005, **88**, 1713.
2. Hanson, B., Learning from natural disasters. *Science*, 2005, **308**, 1125.
3. Lay, T. *et al*., The Great Sumatra–Andaman earthquake of 26 December 2004. *Science*, 2005, **308**, 1127–1133.
4. Bilham, R., A flying start, then a slow slip. *Science*, 2005, **308**, 1126–1127.
5. McCloskey, J., Nalbant, S. S. and Steacy, S., Indonesian earthquake: Earthquake risk from co-seismic stress. *Nature*, 2005, **434**, 291.
6. McNeil, L., Henstock, T. and Tappin, D., The eastern Indian Ocean earthquake and tsunami; First seafloor survey by Royal Navy's *HMS Scott*. *Hydro Int.*, 2005, **9**, 7–9.
7. Prawirodirdjo, L. *et al*., Geodetic observations of interseismic strain segmentation at the Sumatra subduction zone. *Geophys. Res. Lett*., 1997, **24**, 2601–2604.
8. Curray, J. R., Emmel, F. J., Moore, D. G. and Raitt, R. W., Structure, tectonics and geological history of the northeastern Indian Ocean. In *The Ocean Basins and Margins. The Indian Ocean* (eds Nairn, A. E. M. and Stehli, F. G.), Plenum Press, New York, 1982, vol. 6, pp. 399–450.
9. Roy, S. K. and Das Sharma, S., Evolution of Andaman forearc basin and its hydrocarbon potential. In Proceedings of the Second Seminar on Petroliferous Basins of India (ed. Biswas, S. K.), 1993, vol. 1, pp. 407–435.
10. Jade, S., Ananda, M. B., Dileep Kumar, P. and Banerjee, S., Co-seismic and post-seismic displacements in Andaman and Nicobar Islands from GPS measurements. *Curr. Sci.*, 2005, **88**, 1980–1984.

ACKNOWLEDGEMENTS. The Department of Ocean Development, New Delhi provided a grant for the seabed survey under Exclusive Economic Zone (EEZ) of India project (GAP 1438). We thank H. K. Gupta and S. R. Shetye, NIO, Goa for taking keen interest in the expedition, and the Director, NCAOR for vessel support. The EEZ project colleagues are thanked for help during on-board data collection and processing. This is NIO contribution 4091.

Received 7 June 2005; revised accepted 20 January 2006

Physical parameters of hydrated sediments estimated from marine seismic reflection data

Ranjana Ghosh, Maheswar Ojha, Kalachand Sain* and N. K. Thakur

National Geophysical Research Institute, Uppal Road, Hyderabad 500 007, India

Gas-hydrates in marine sediments can be identified on multi-channel seismic data by an anomalous bottom simulating reflector (BSR), often associated with the base of hydrate stability field. Physical parameters like porosity, density, thermal conductivity, temperature, geothermal gradient, hydrate saturation, electrical resistivity and heat flow provide useful inputs to understand several issues related to hydrates exploration. To determine these parameters by employing relevant techniques at depth below the sea water is not only difficult but also expensive. Here, we present case studies to derive these parameters with the help of BSR, identified on seismic sections from two completely different tectonic/geological areas of (i) the Makran (Arabian Sea) and (ii) the Cascadia (Pacific Ocean) margins. From the available velocity–depth model in the Cascadia margin, we determine the background velocity–depth function (without hydrates and free-gas), which is used to estimate the variation of density, porosity and hydrate saturation with depth successively. The average bulk density, seafloor porosity and maximum hydrate saturation in the Cascadia margin are calculated as 1.70 g/cc, 63.8% and 22% respectively. From the porosity–depth function and the gradient of hydrate saturation, we determine the variation of thermal conductivity and resistivity with depth. The average resistivity, thermal conductivity and heat flow in the Cascadia margin are determined as 1.13 Ω-m, 0.58 W/m/K and 62.85 mW/m^2 respectively. Since the velocity model in the Makran accretionary prism across the BSR shows wide variation, we change the approach of deriving the above physical parameters. First, we determine the seafloor density from the seismic velocity and hence the seafloor porosity. Then the porosity–depth function is determined using Athy's law and the compaction factor available for the sediment. Porosity is then converted into density using an empirical relation between porosity and density. The remaining procedure is the same as that used for the Cascadia margin. Seafloor porosity, average density, resistivity, thermal conductivity, heat flow and maximum hydrate saturation are calculated as 54%, 1.98 g/cc, 1.96 Ω-m, 1.268 W/m/K, 43.55 mW/m^2 and 13% respectively, for the Makran region. The estimated physical parameters in both the margins match well with the available results. We also estimate errors

*For correspondence. (e-mail: kalachandsain@yahoo.com)